*Electronic Supplementary Material (ESI) for Physical Chemistry Chemical Physics Journal*

# Thermally stable J-type phthalocyanine dimers as new non-linear absorbers for low-threshold optical limiters

Alexander Yu. Tolbin,[a] Mikhail S. Savelyev,[b] Alexander Yu. Gerasimenko,[b] Larisa G. Tomilova[a,c] and Nikolay S. Zefirov[a,c]

[a] Institute of Physiologically Active Compounds, Russian Academy of Sciences, 142432 Chernogolovka, Moscow Region (Russian Federation)
[b] National Research University of Electronic Technology, 124498 Moscow, Zelenograd (Russian Federation)
[c] Department of Chemistry M. V. Lomonosov Moscow State University, 119991 Moscow (Russian Federation)

* Corresponding author. Tel.: +7 496 5242566, e-mail address: tolbin@ipac.ac.ru (Prof. A.Yu. Tolbin).

## Table of Contents

# 1. MALDI-TOF mass spectra

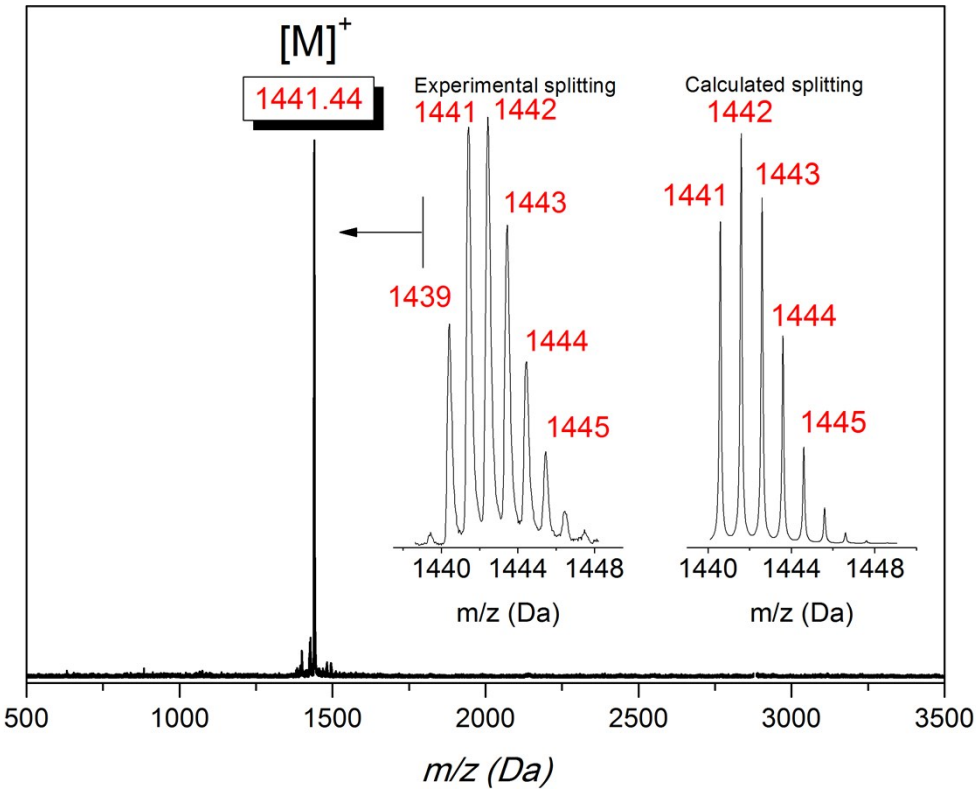


**Fig. S1**. MALDI-TOF mass spectrum of Compound **2a**.

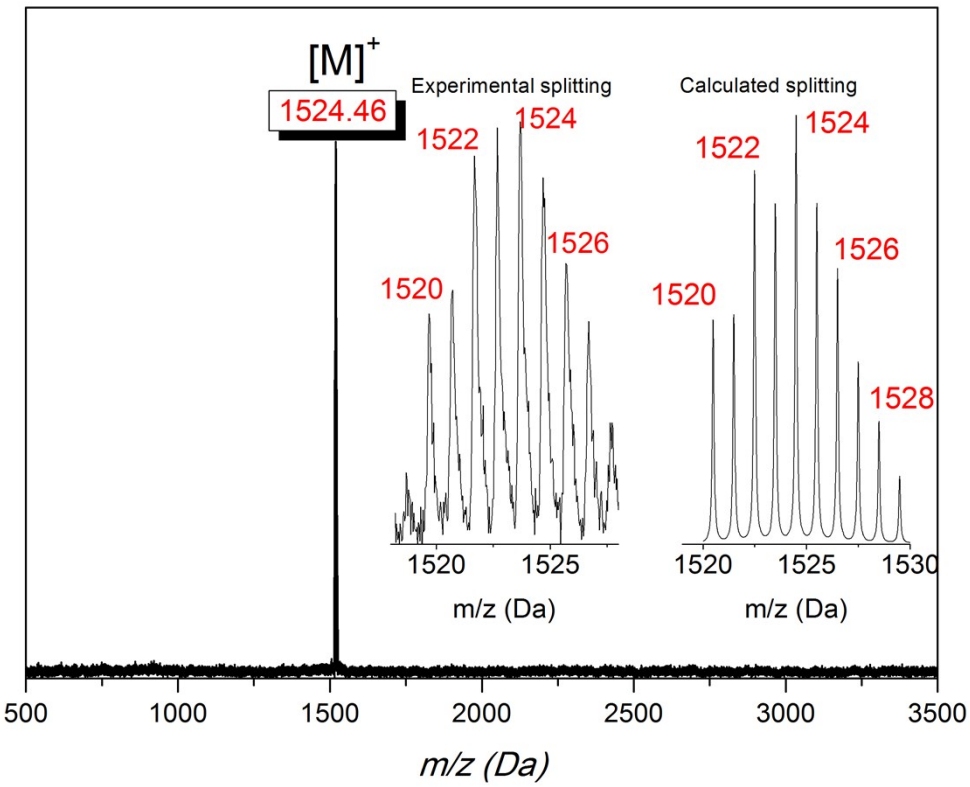


**Fig. S2**. MALDI-TOF mass spectrum of Compound **2b**.

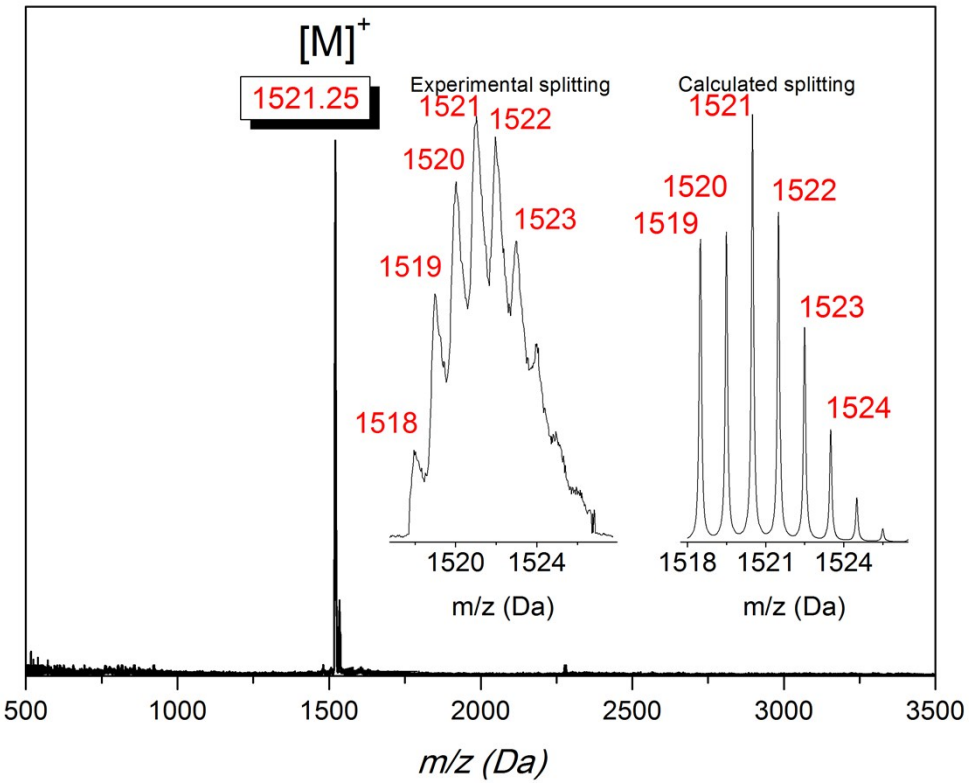


**Fig. S3**. MALDI-TOF mass spectrum of Compound **2c**.

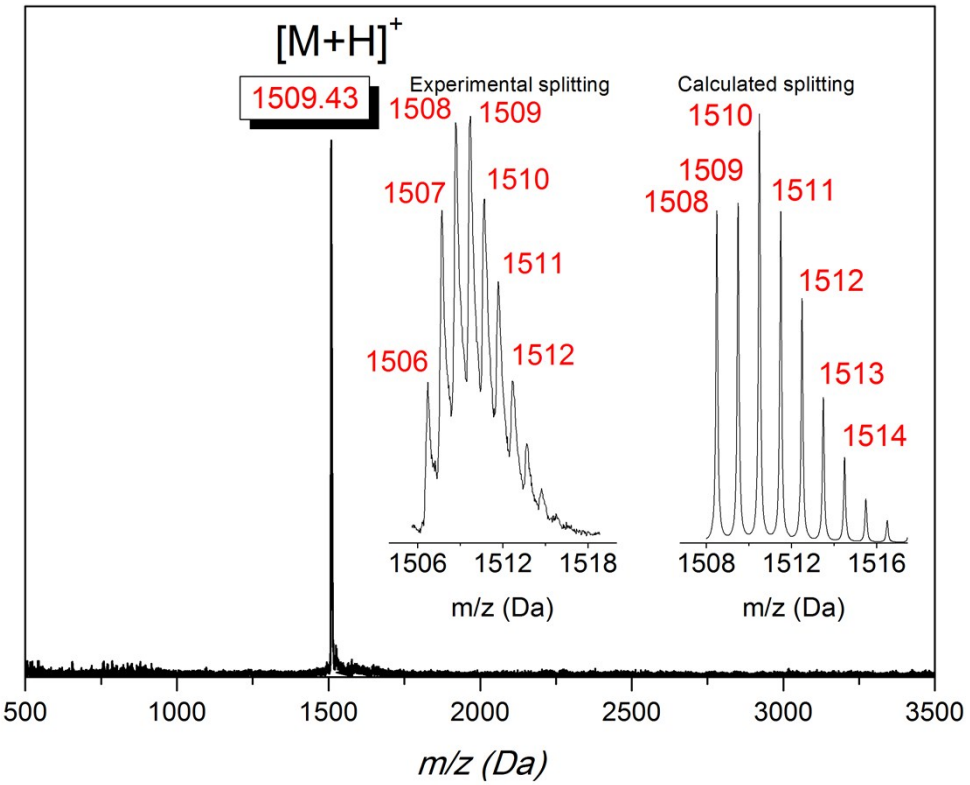


**Fig. S4**. MALDI-TOF mass spectrum of Compound **2d**.

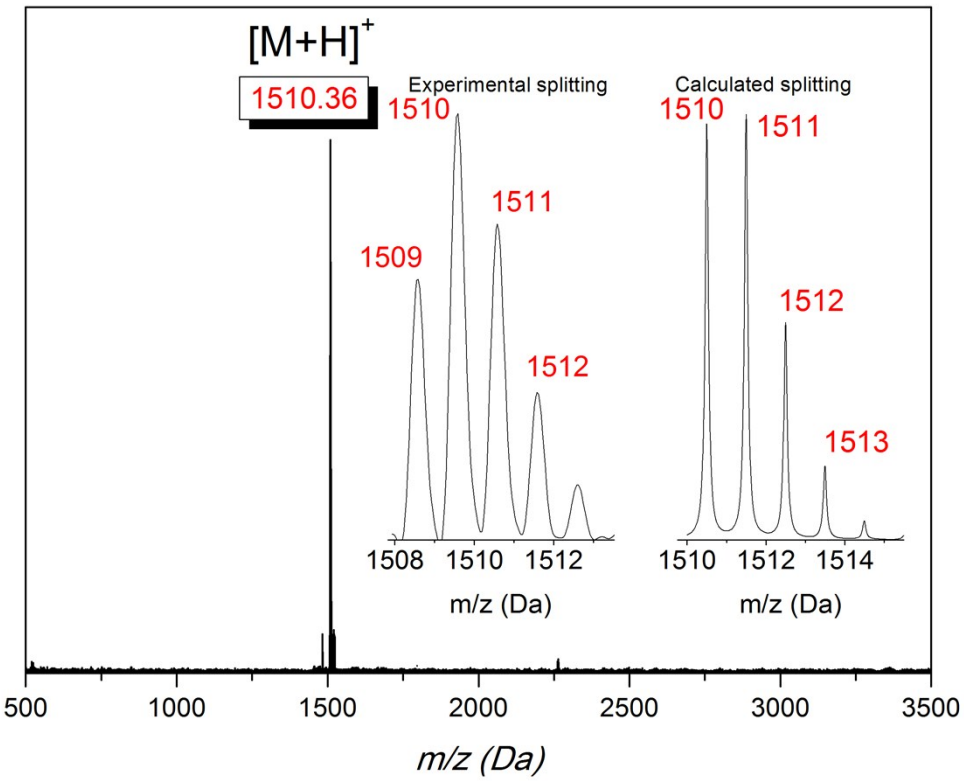


**Fig. S5**. MALDI-TOF mass spectrum of Compound **2e**.

# 2. Proton NMR spectra

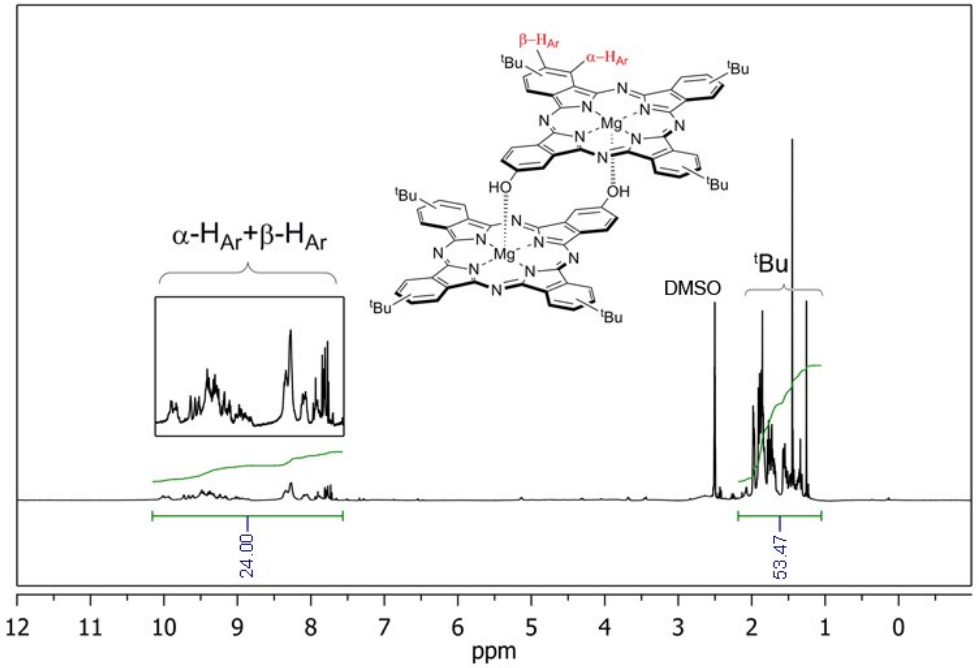


**Fig. S6**. $^{1}$H NMR spectrum ($CCl_4$+5%DMSO-$d_6$; 333K, 500MHz) of Compound **2a**.

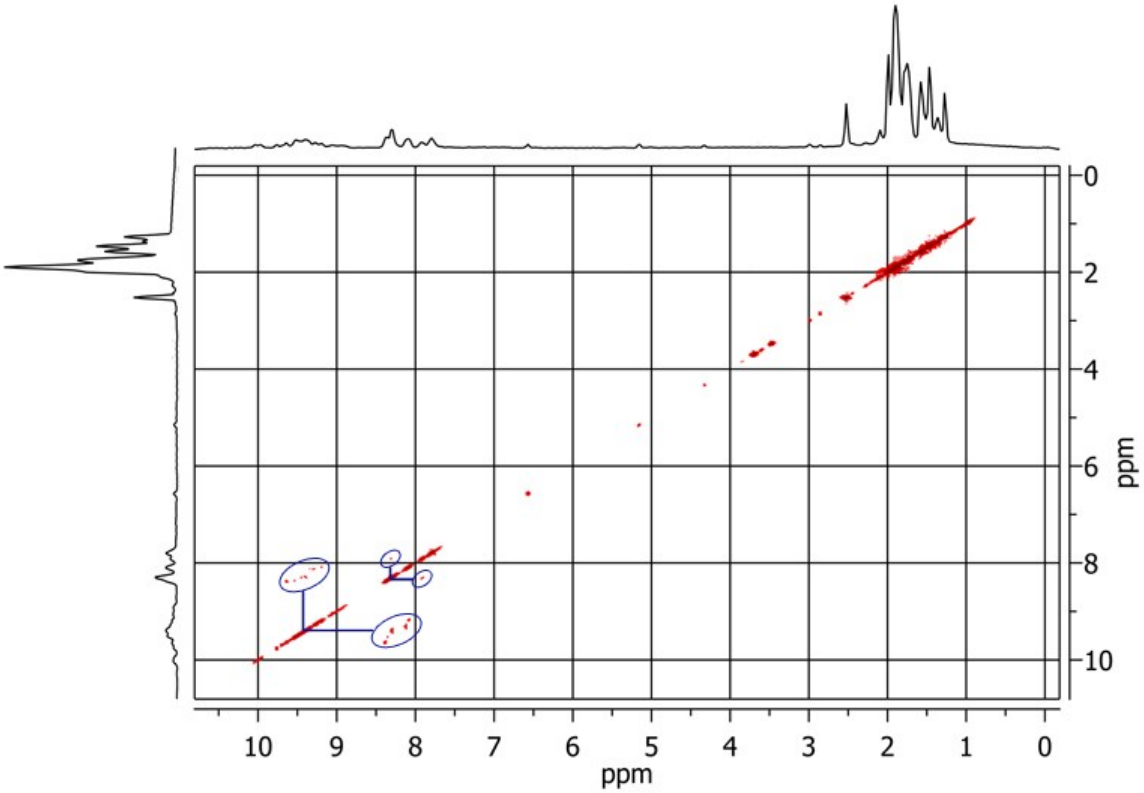


**Fig. S7**. $^{1}H–^{1}H$ COSY NMR spectrum ($CCl_4$+5%DMSO-$d_6$; 333K, 500MHz) of Compound **2a**.

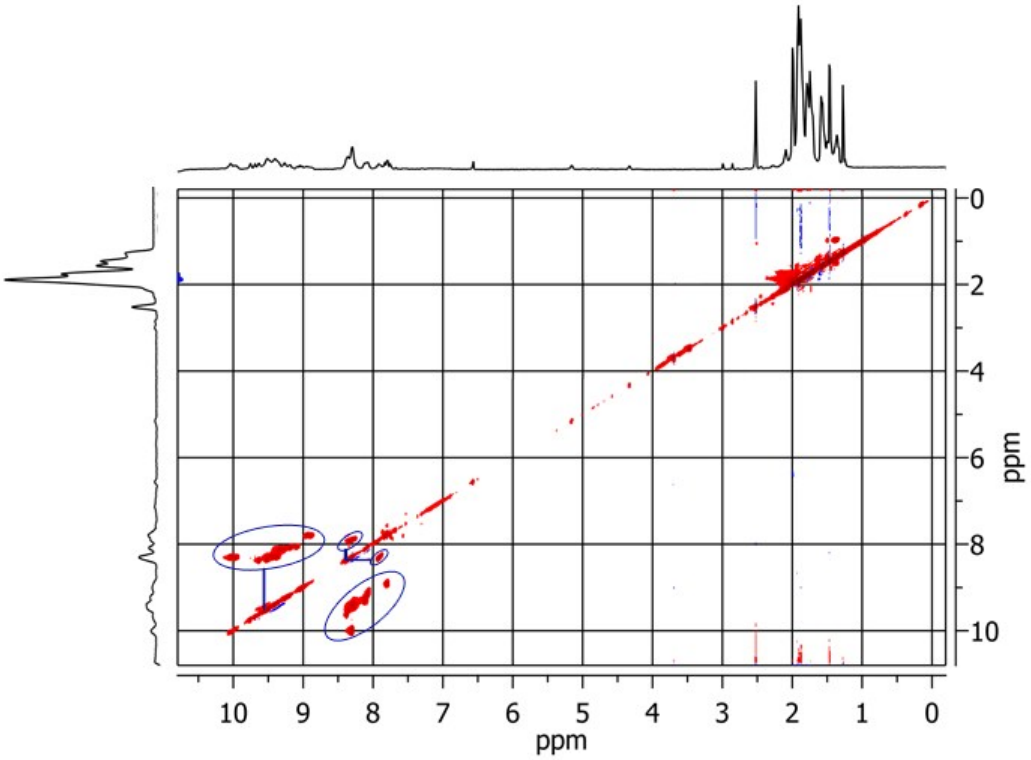


**Fig. S8**. $^{1}H–^{1}H$ TOCSY NMR spectrum ($CCl_4$+5%DMSO-$d_6$; 333K, 500MHz) of Compound **2a**.

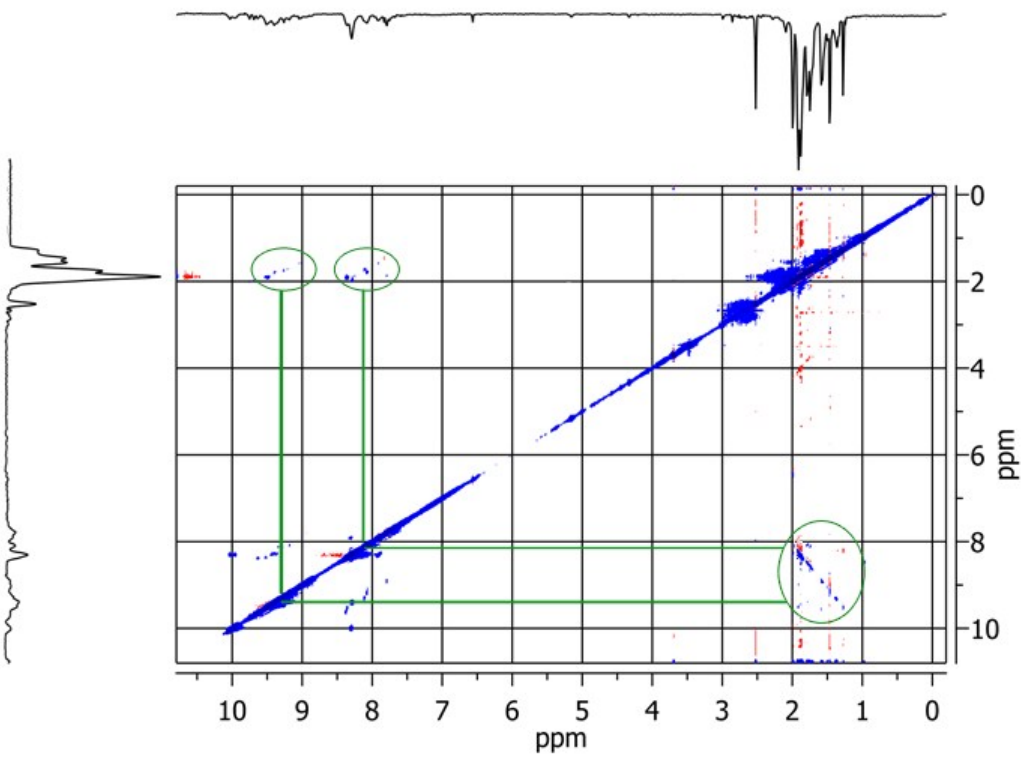


**Fig. S9**. $^{1}H–^{1}H$ NOESY NMR spectrum ($CCl_4$+5%DMSO-$d_6$; 333K, 500MHz) of Compound **2a**.

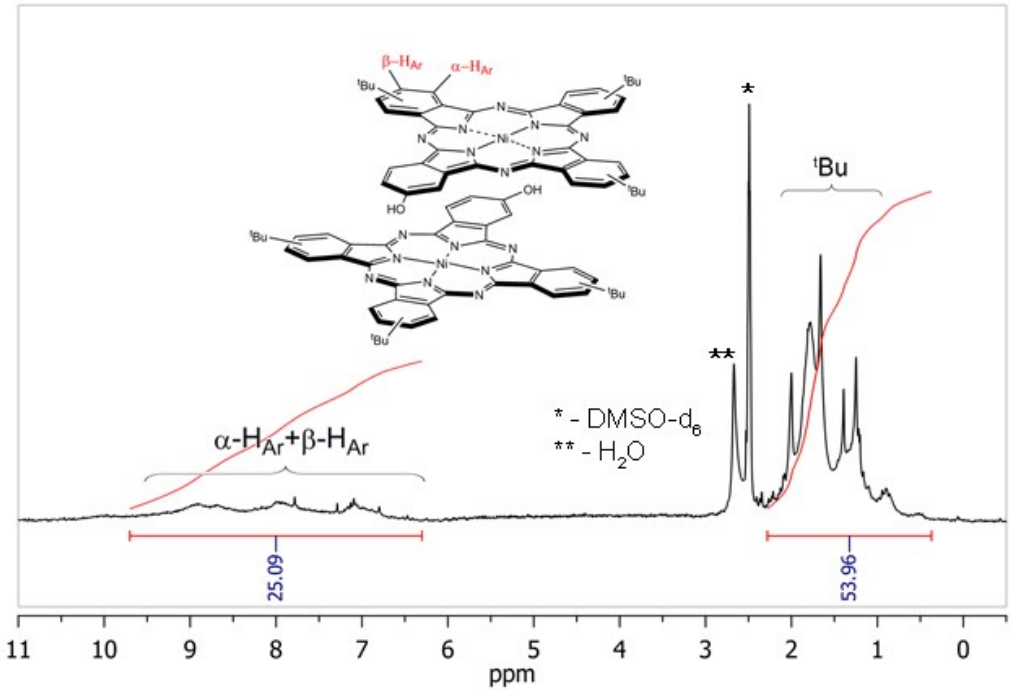


**Fig. S10**. $^{1}H$ NMR spectrum ($CCl_4$+5%DMSO-$d_6$; 298K, 200MHz) of Compound **2d**.

# 3. UV/Vis Spectra

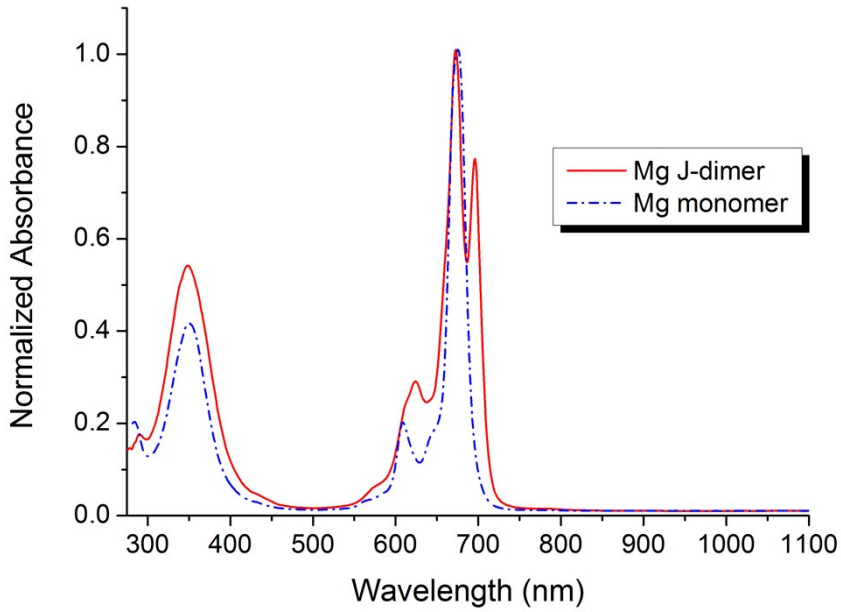


**Fig. S11**. UV/Vis spectra of J-dimer (Compound **2a**) and corresponding monomer in THF (C~$1.2\times10^{-5}$mol $dm^{-3}$).

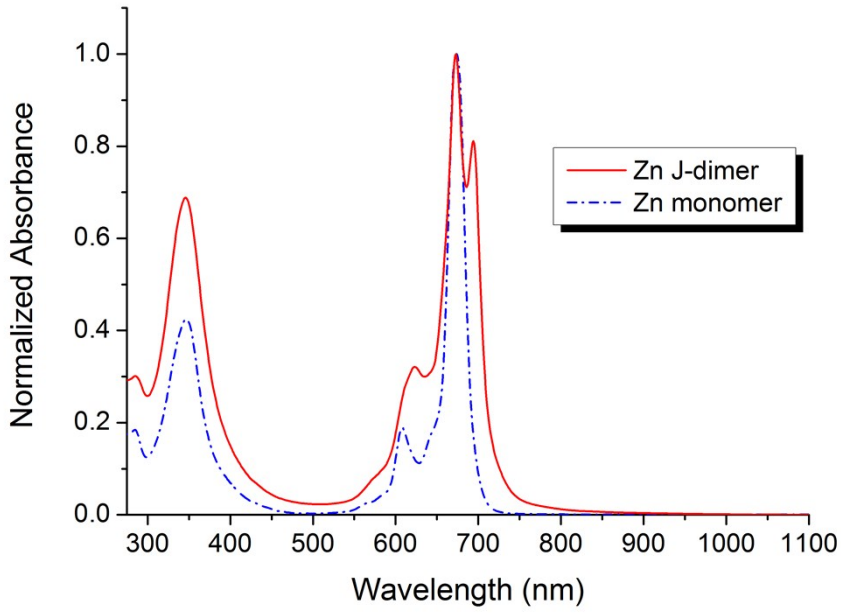


**Fig. S12**. UV/Vis spectra of J-dimer (Compound **2b**) and corresponding monomer in THF (C~$1.2\times10^{-5}$mol $dm^{-3}$).

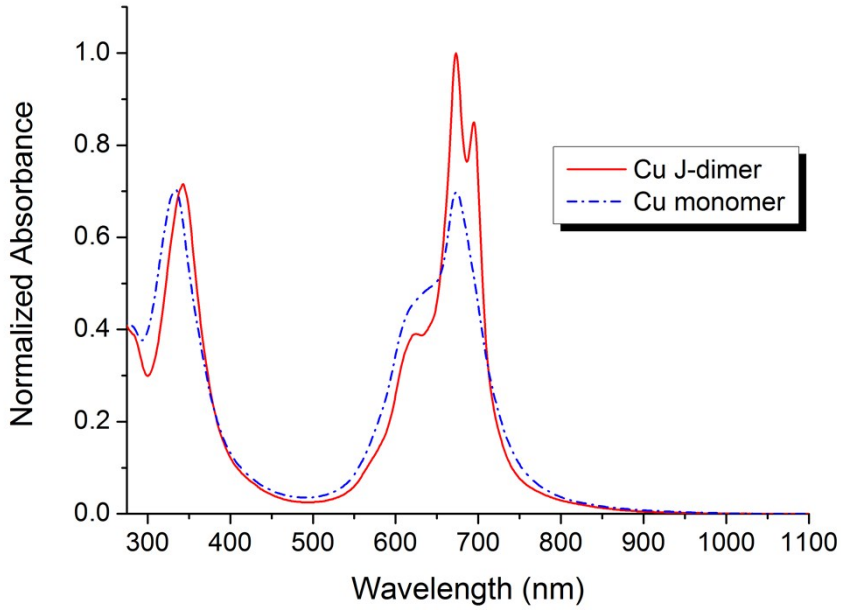


**Fig. S13**. UV/Vis spectra of J-dimer (Compound **2c**) and corresponding monomer in THF (C~$1.2\times10^{-5}$mol $dm^{-3}$). As can be seen, copper monomer has a tendency to form H-aggregates even in medium polar solvents.

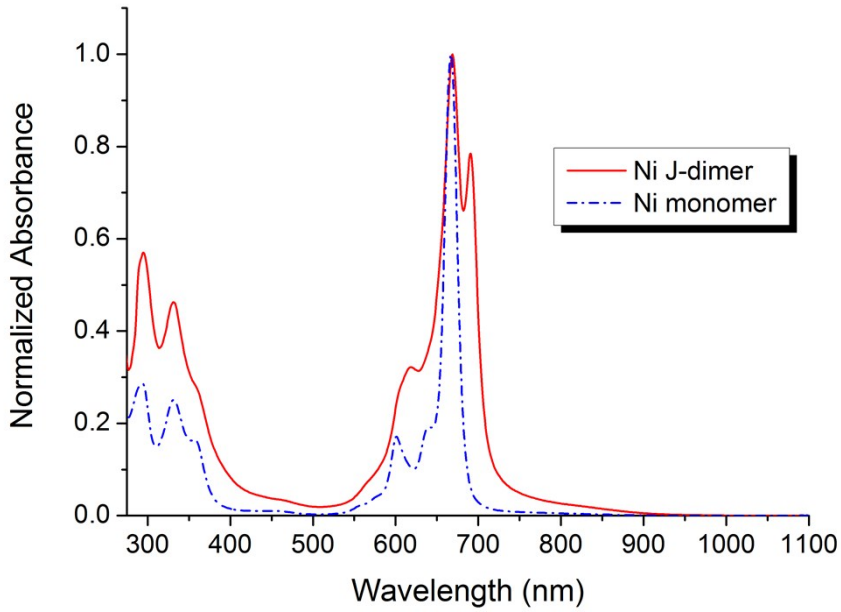


**Fig. S14**. UV/Vis spectra of J-dimer (Compound **2d**) and corresponding monomer in THF (C~$1.2\times10^{-5}$mol $dm^{-3}$).

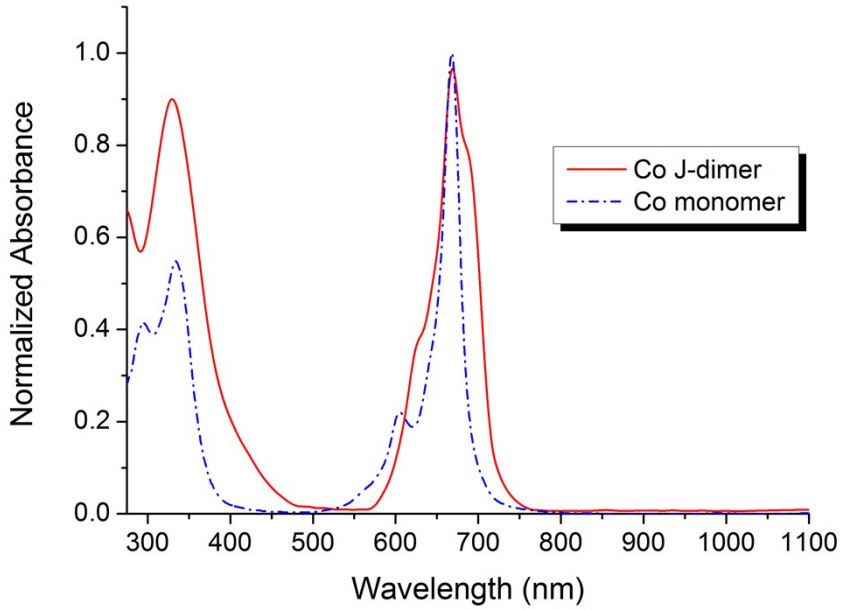


**Fig. S15**. UV/Vis spectra of J-dimer (Compound **2e**) and corresponding monomer in THF (C~1.2×10$^{-5}$mol dm$^{-3}$).

# 4. Fluorescence study

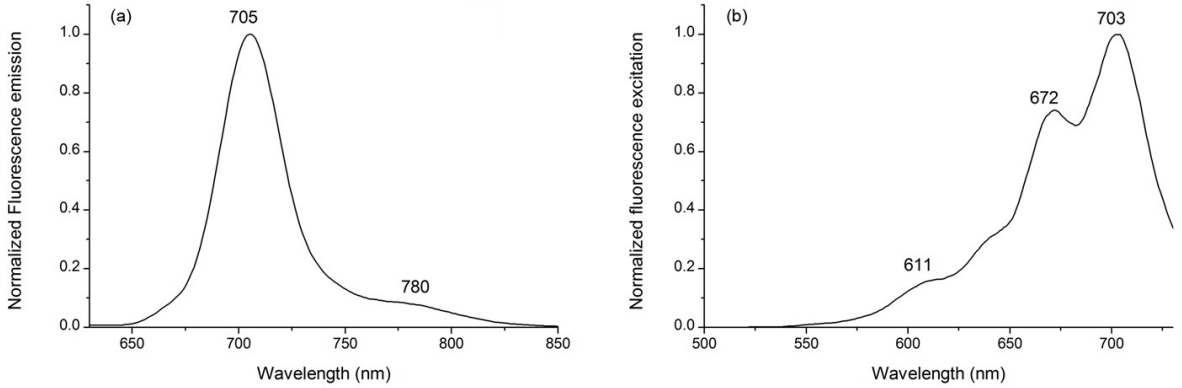


**Fig. S16**. Fluorescence emission (a) /$\lambda_{exc}$=600 nm/ and excitation /$\lambda_{em}$=750 nm/ (b) spectra of Compound **2a**.

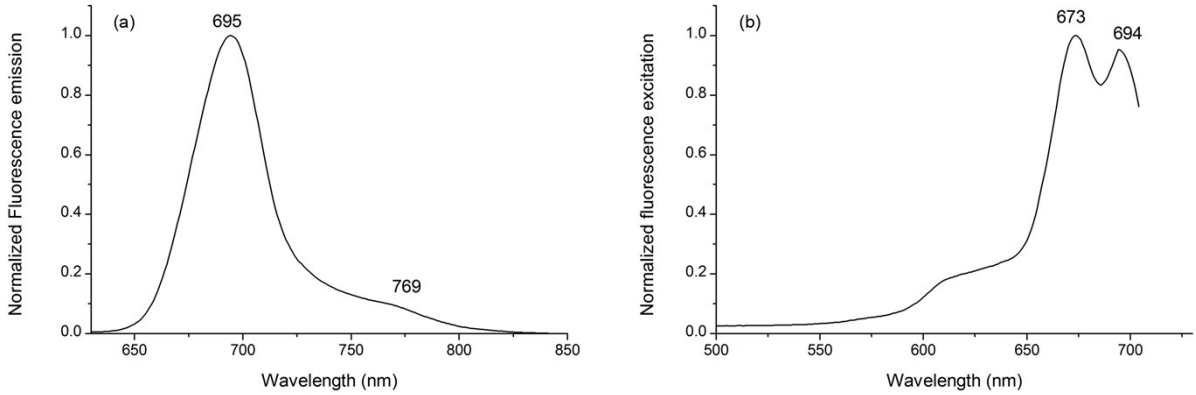


**Fig. S17**. Fluorescence emission (a) /$\lambda_{exc}$=600 nm/ and excitation /$\lambda_{em}$=750 nm/ (b) spectra of Compound **2b**.

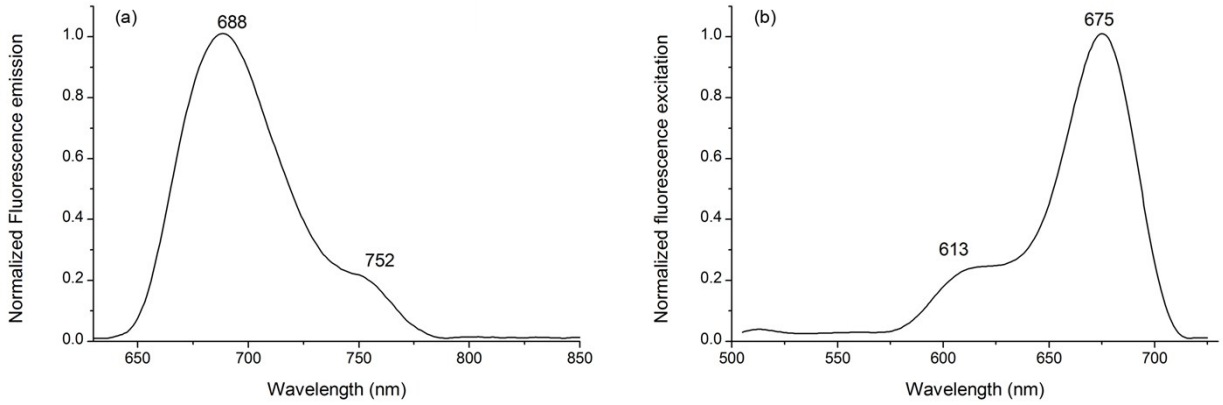


**Fig. S18**. Fluorescence emission (a) /$\lambda_{exc}$=600 nm/ and excitation /$\lambda_{em}$=750 nm/ (b) spectra of Compound **2c**.

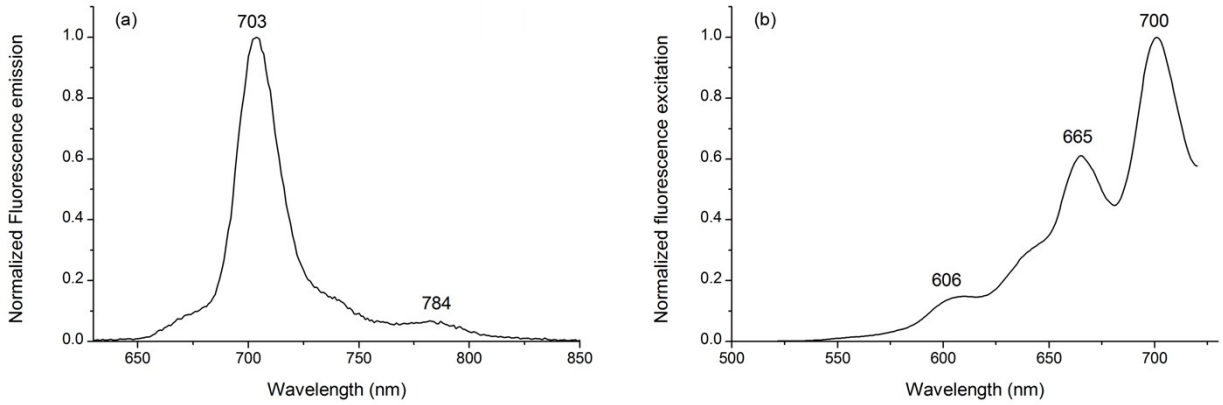


**Fig. S19**. Fluorescence emission (a) /$\lambda_{exc}$=600 nm/ and excitation /$\lambda_{em}$=750 nm/ (b) spectra of Compound **2d**.



**Fig. S20**. Fluorescence emission (a) /$\lambda_{exc}$=600 nm/ and excitation /$\lambda_{em}$=750 nm/ (b) spectra of Compound **2e**.

# 5. Details on "Threshold" model

In the case of *Z*-scan the incident laser pulse intensity $I_0(\rho,\varphi,z,t)$ of Gaussian type can be represented as follows:

$$I_0(\rho,\varphi,z,t)=\frac{2U_0}{w^2(z)\tau\pi\sqrt{\pi}}\exp\left(-\frac{2\rho^2}{w^2(z)}\right)\exp\left(-\frac{t^2}{\tau^2}\right), \quad (1)$$

where $U_0$ is the total pulse energy, $(\rho,\varphi)$ are the polar coordinates in the cross section of the laser beam, $\tau$ is the pulse width, $z$ is the sample displacement relative to the beam waist, $t$ is the time, $w$ is the beam radius. The dependence between radial pulse profile in a section of the laser beam and distance from the axis of the laser beam $\rho$ is rotationally symmetric.

When a lens near the beam waist focuses the beam, the radius can be written as:

$$w^2(z)=w_0^2\left(\frac{z_0^2+z^2}{z_0^2}\right), \tag{2}$$

where $z_0=\frac{\pi w_0^2}{\lambda}$, $\lambda$ is a wavelength of the laser radiation and $w_0$ is the beam radius in the waist by the level of $1/e^2$.

The solution of the nonlinear radiative transfer equation (RTE) for "threshold" model can be written in implicit view:

for $I_c > I_0(\rho,\varphi,z,t)$, $I_0(\rho,\varphi,z,t) > I(\rho,\varphi,z,t,d)$, $I_c > I(\rho,\varphi,z,t,d)$:

$$\int_{I_0(\rho,\varphi,z,t)}^{I(\rho,\varphi,z,t,d)}\frac{dI}{I\alpha}=-d\,, \tag{3}$$

for $I_0(\rho,\varphi,z,t) > I_c$, $I_0(\rho,\varphi,z,t) > I(\rho,\varphi,z,t,d)$, $I_c > I(\rho,\varphi,z,t,d)$:

$$\int_{I_c}^{I(\rho,\varphi,z,t,d)}\frac{dI}{I\alpha}+\int_{I_0(\rho,\varphi,z,t)}^{I_c}\frac{dI}{I(\alpha-\beta I_c+\beta I)}=-d\,, \tag{4}$$

for $I_0(\rho,\varphi,z,t) > I_c$, $I(\rho,\varphi,z,t,d) > I_c$, $I_0(\rho,\varphi,z,t) > I(\rho,\varphi,z,t,d)$:

$$\int_{I_0(\rho,\varphi,z,t)}^{I(\rho,\varphi,z,t,d)}\frac{dI}{I(\alpha-\beta I_c+\beta I)}=-d\,. \tag{5}$$

The solution of $I(\rho,\varphi,z,t,d)$ for the RTE was found on the basis of relations (3-5):

$$\begin{aligned} I(\rho,\varphi,z,t,d) &= \eta(I_c-I_0(\rho,\varphi,z,t))I_0(\rho,\varphi,z,t)\exp(-\alpha d)+\\ &+\eta(I_0(\rho,\varphi,z,t)-I_c)\eta(I_1-I_0(\rho,\varphi,z,t))\frac{I_c}{\exp(\alpha d)}\left(\frac{\alpha I_0(\rho,\varphi,z,t)}{(\alpha-\beta_c I_c+\beta_c I_0(\rho,\varphi,z,t))I_c}\right)^{\frac{\alpha}{\alpha-\beta_c I_c}}+\\ &+\eta(I_0(\rho,\varphi,z,t)-I_c)\eta(I_0(\rho,\varphi,z,t)-I_1)\frac{(\alpha-\beta_c I_c)I_0(\rho,\varphi,z,t)\exp(-[\alpha-\beta_c I_c]d)}{\alpha-\beta_c I_c+\beta_c I_0(\rho,\varphi,z,t)(1-\exp(-[\alpha-\beta_c I_c]d))} \end{aligned}, \tag{6}$$

where $I_1=\frac{(\alpha-\beta_c I_c)I_c}{\alpha\exp(-[\alpha-\beta_c I_c]d)-\beta_c I_c}$, it follows from the condition $I_c=I(\rho,\varphi,z,t,d)$.

The input fluence of the laser pulse is equal:

$$F_0(\rho,\varphi,z)=U_0\frac{2}{w^2(z)\pi}\exp\left(-\frac{2\rho^2}{w^2(z)}\right). \tag{7}$$

The output fluence of the laser pulse was determine by following equation:

$$F(\rho,\varphi,z,d)=(I_c-I_0(\rho,\varphi,z,t))\int_{-\infty}^{\infty}I_0(\rho,\varphi,z,t)\exp(-\alpha d)dt+$$

$$+\eta(I_0(\rho,\varphi,z,t)-I_c)\eta(I_1-I_0(\rho,\varphi,z,t))\int_{-\infty}^{\infty}\frac{I_c}{\exp(\alpha d)}\left(\frac{\alpha I_0(\rho,\varphi,z,t)}{(\alpha-\beta_c I_c+\beta_c I_0(\rho,\varphi,z,t))I_c}\right)^{\frac{\alpha}{\alpha-\beta_c I_c}}dt+ \quad (8)$$

$$+\eta(I_0(\rho,\varphi,z,t)-I_c)\eta(I_0(\rho,\varphi,z,t)-I_1)\int_{-\infty}^{\infty}\frac{(\alpha-\beta_c I_c)I_0(\rho,\varphi,z,t)\exp(-[\alpha-\beta_c I_c]d)}{\alpha-\beta_c I_c+\beta_c I_0(\rho,\varphi,z,t)(1-\exp(-[\alpha-\beta_c I_c]d))}dt$$

The final expression for the output fluence was obtained after substituting $I_0(\rho,\varphi,z,t)=U_0\frac{2}{w^2(z)\pi\pi^{3/2}}\exp\left(-\frac{2\rho^2}{w^2(z)}\right)\exp\left(-\frac{t^2}{\tau^2}\right)$ and integration of equation (8):

$$F(\rho,\varphi,z,d)=U_0\frac{2}{w^2(z)\pi}\exp(-\alpha d)\exp\left(-\frac{2\rho^2}{w^2(z)}\right)\left[1-\frac{2}{\sqrt{\pi}}\eta(\gamma-1)\mathrm{ls}_0\left(0,1,\sqrt{\ln(\gamma)}\right)+\right.$$

$$+\frac{2}{\gamma\sqrt{\pi}}\left(\frac{\gamma}{1-\xi}\right)^{\frac{1}{1-\xi}}\eta(\gamma-1)\mathrm{ls}_0\left(\frac{\xi\gamma}{1-\xi},\frac{1}{1-\xi},\sqrt{\ln(\gamma)}\right)-$$

$$-\frac{2}{\gamma\sqrt{\pi}}\left(\frac{\gamma}{1-\xi}\right)^{\frac{1}{1-\xi}}\eta(\gamma-1)\eta(\gamma_1-1)\mathrm{ls}_0\left(\frac{\xi\gamma}{1-\xi},\frac{1}{1-\xi},\sqrt{\ln(\gamma_1)}\right)+ \quad (9)$$

$$\left.+\frac{2}{\sqrt{\pi}}\eta(\gamma-1)\eta(\gamma_1-1)\exp(\alpha\xi d)\mathrm{ls}_0\left(\frac{\xi\gamma}{1-\xi}(1-\exp(-\alpha[1-\xi]d)),1,\sqrt{\ln(\gamma_1)}\right)\right]$$

where $\gamma=\frac{2U_0}{I_c w^2(z)\pi(\pi)^{3/2}}\exp\left(-\frac{2\rho^2}{w^2(z)}\right)$, $\gamma_1=\frac{2U_0}{I_1 w^2(z)\pi(\pi)^{3/2}}\exp\left(-\frac{2\rho^2}{w^2(z)}\right)$, $\xi=\frac{\beta I_c}{\alpha}$ and we introduced a function:

$$\mathrm{ls}_0(a,b,c)=\int_0^c\left(\frac{\exp(-r^2)}{1+a\exp(-r^2)}\right)^b dr. \quad (10)$$

Function to approximate the theoretical values of the attenuation coefficient is:

$$T(z,d)=\frac{\int_0^{2\pi}\int_0^{\infty}F(\rho,\varphi,z,d)\rho d\rho d\varphi}{\int_0^{2\pi}\int_0^{\infty}F_0(\rho,\varphi,z)\rho d\rho d\varphi}\exp(\alpha d). \quad (11)$$

Since the dependence between radial pulse profile in a section of the laser beam and distance from the axis of the laser beam is rotationally symmetric. We can write:

$$T(z,d)=\frac{\int_0^{\infty} F(\rho,z,d)\rho d\rho}{\int_0^{\infty} F_0(\rho,z)\rho d\rho}\exp(\alpha d). \qquad (12)$$

As an example we demonstrate the accuracy of approximation of experimental data for J-dimer **2a**:

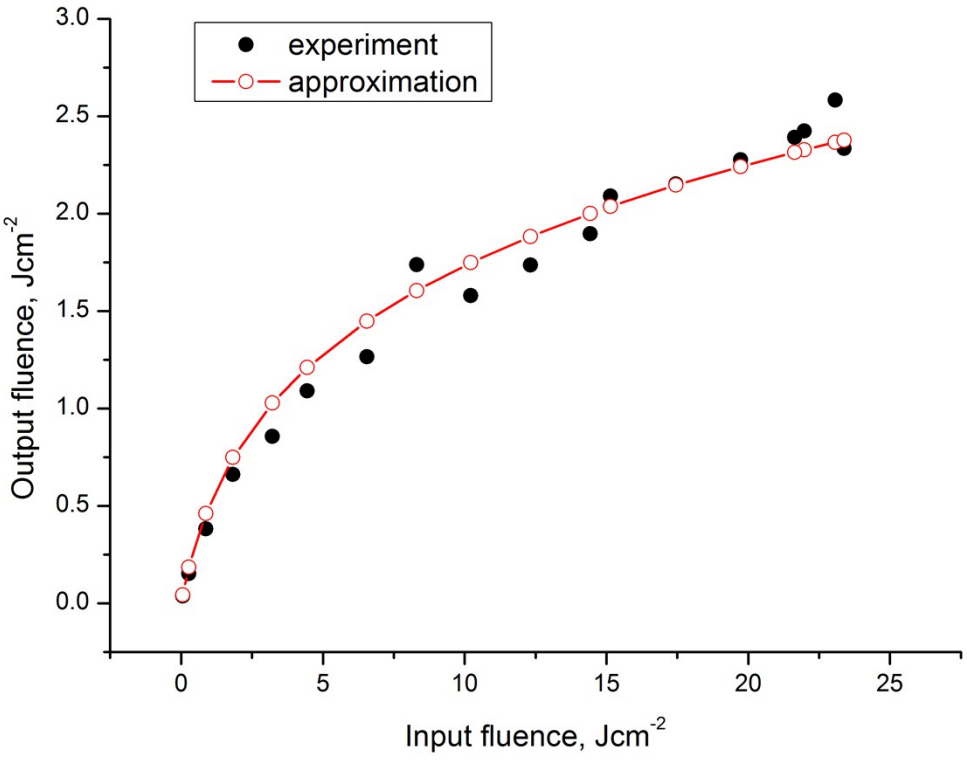


**Fig. S21**. Optical limiting curve for J-dimer **2a** - experiment and approximation with function *T(z,d)* (Equation - 12).